Cyclocreatine Suppresses Creatine Metabolism and Impairs Prostate Cancer Progression

Rachana Patel[1], Catriona A. Ford[1], Lisa Rodgers[1,2], Linda K. Rushworth[1,2], Janis Fleming[1], Ernest Mui[1,2], Tong Zhang[3], David Watson[3], Victoria Lynch[4], Gillian Mackay[1], David Sumpton[1], Owen J. Sansom[1,2], Johan Vande Voorde[1], and Hing Y. Leung[1,2]

ABSTRACT

Prostate cancer is the second most common cause of cancer mortality in men worldwide. Applying a novel genetically engineered mouse model (GEMM) of aggressive prostate cancer driven by deficiency of the tumor suppressors PTEN and Sprouty2 (SPRY2), we identified enhanced creatine metabolism as a central component of progressive disease. Creatine treatment was associated with enhanced cellular basal respiration *in vitro* and increased tumor cell proliferation *in vivo*. Stable isotope tracing revealed that intracellular levels of creatine in prostate cancer cells are predominantly dictated by exogenous availability rather than by *de novo* synthesis from arginine. Genetic silencing of creatine transporter *SLC6A8* depleted intracellular creatine levels and reduced the colony-forming capacity of human prostate cancer cells. Accordingly, *in vitro* treatment of prostate cancer cells with cyclocreatine, a creatine analog, dramatically reduced intracellular levels of creatine and its derivatives phosphocreatine and creatinine and suppressed proliferation. Supplementation with cyclocreatine impaired cancer progression in the PTEN- and SPRY2-deficient prostate cancer GEMMs and in a xenograft liver metastasis model. Collectively, these results identify a metabolic vulnerability in prostate cancer and demonstrate a rational therapeutic strategy to exploit this vulnerability to impede tumor progression.

Significance: Enhanced creatine uptake drives prostate cancer progression and confers a metabolic vulnerability to treatment with the creatine analog cyclocreatine.

Introduction

Prostate cancer is the most common cancer in men worldwide (1). Around 20% of patients present with advanced disease at the time of diagnosis. Even for men found to have an early or indolent form of the disease, at least 20% of these patients will subsequently progress to a lethal and treatment-resistant form of prostate cancer (2). Therefore, identification and characterization of genetic lesions that influence aggressive prostate cancer growth may provide new strategies to improve clinical management of disease progression. We have previously shown that genomic loss of the tumor suppressors PTEN and Sprouty2 (SPRY2) co-occur in progressive prostate cancers including in treatment resistance (3–5), and that concurrent loss of PTEN and SPRY2 leads to aggressive treatment-resistant disease (3–5).

Oncogenic metabolic rewiring mediated by loss of tumor suppressors is one of the hallmarks of cancer (6). Aggressive cancers have high energy demands and may experience nutrient restricting conditions during rapid proliferative stages of tumorigenesis (7). Identifying and understanding metabolic rewiring triggered by loss of tumor suppressors may provide new insights to target cancer growth and invasion.

The phosphagen system refers to high energy storage compounds and associated biosynthesis enzymes (8–10). This cellular buffering system comprises of creatine, a nitrogen amine that can be phosphorylated by creatine kinases to form phosphocreatine. In addition to uptake of creatine from circulation, creatine can also be synthesised *de novo* from arginine and glycine, with S-adenosyl methionine serving as the methyl donor (11). Creatine kinases play a central role in the energy metabolism of cells that have high and fluctuating energy requirements by catalyzing the reversible transfer of the phosphoryl group from phosphocreatine to ADP to generate ATP (12). Phosphocreatine serves as an easily diffusible energy storage metabolite to regenerate ATP on demand by cytosolic creatine kinase isoforms. It has previously been shown that the phosphagen system is exploited by breast cancer cells to meet their high energy demands (13), and that creatine can affect SMAD2/3 phosphorylation in colorectal cancer to promote metastasis (14). Also, heterocyclic aromatic amines, derived from creatine and other dietary sources following cooking at high temperatures, have been associated with increased cancer risk for multiple cancer types including colorectal and prostate cancers (15–17).

The role of creatine metabolism in prostate cancer has not been fully explored. Here, we used clinically relevant human and murine prostate cancer models to investigate the role of combined PTEN and SPRY2 deficiency in mediating metabolic reprogramming of prostate cancer cells. Our data point to creatine uptake as a vulnerability of progressive prostate cancer. This is of particular relevance given that dietary creatine supplementation has been implicated to have multiple health benefits, including potential anticancer activities (18). In patients with prostate cancer receiving androgen deprivation therapy, creatine supplementation has been suggested to enhance the positive effects of resistance training on patient performance and quality of life (19, 20).

[1]CRUK Beatson Institute, Glasgow, United Kingdom. [2]Institute of Cancer Sciences, University of Glasgow, Glasgow, United Kingdom. [3]Strathclyde Institute of Pharmacy and Biomedical Sciences, University of Strathclyde, Glasgow, United Kingdom. [4]Department of Histopathology, Queen Elizabeth University Hospital, Glasgow, United Kingdom.

Note: Supplementary data for this article are available at Cancer Research Online (http://cancerres.aacrjournals.org/).

R. Patel and C.A. Ford contributed equally to this article.

Corresponding Authors: Hing Y. Leung and Johan Vande Voorde, CRUK Beatson Institute, Garscube Estate, Switchback Road, Bearsden, Glasgow G611BD, United Kingdom. Phone: 44-0-141-330-3953; E-mail: h.leung@beatson.gla.ac.uk and j.vandevoorde@beatson.gla.ac.uk

Cancer Res 2022;82:2565–75

doi: 10.1158/0008-5472.CAN-21-1301

Materials and Methods

Mice

All animal experiments were carried out with ethical approval from the University of Glasgow under the revised Animal (Scientific Procedures) Act 1986 and the EU Directive 2010/63/EU (PPL P5EE22AEE). The ARR2Probasin-Cre (Pb-Cre), *Pten*^{flox}, *Spry2*^{flox} (4, 5) mice have been previously described, and applied to generate the *Pten*$^{pc-/-}$ *Spry2*$^{pc-/-}$ experimental cohort. All mice in this study were on a mixed background and were genotyped by Transnetyx using PCR analysis of ear notch tissue. Mice were housed at 19°C to 23°C with a 12-hour light–dark cycle, and were fed a conventional diet with water *ad libitum*. They were housed in an enriched environment, with igloos, cardboard tubes and chewing sticks. Genotype-specific male mice were handled and aged until experimental time-points or ethically approved clinical endpoints. The total prostate dry weights were used for comparative analysis.

To investigate the effects of creatine on *in vivo* prostate tumors, creatine (40 mg daily; Sigma #C0780) was administered via gavage of 1% creatine solution for 2 months. Similarly, 1% cyclocreatine (w/v; 2-imino-1-imidazolidineaceticacid; Sigma #377627) was supplied in drinking water *ad libitum* for 1 month.

CD-1 nude mice (6–8 weeks old; male) were used to study metastatic tumor cell growth in the liver following splenic injection of PC3M cells (5 million cells per injection into the spleen of each experimental mouse). One percent cyclocreatine (w/v; 2-imino-1-imidazolidineaceticacid; Sigma #377627) in drinking water was started one week after tumor cell implantation *ad libitum* for 1 month. The PREPARE guidelines were used to design and execute experiments. Tumor burden in the liver was assessed at necropsy by inspection for visible tumor lesions, and the number of hepatic lobes involved was used to calculate the percentage involvement. The presence or absence of metastasis in each lobe was then confirmed histologically by hematoxylin and eosin staining.

Cell lines

Human PC3 and PC3M cells were purchased from ATCC. PC3M cells are a metastasis-derived variant of human prostate cancer PC3 cells. Cell lines were *Mycoplasma* negative and authenticated by LGC Standards. P1 murine prostate cancer cells (RRID:CVCL_VQ82) were derived from a prostate tumor from a mouse bearing *Pten*$^{pc-/-}$ tumor at 14 months. Similarly. SP1 and SP2 cell lines (RRID:CVCL_VQ84; RRID:CVCL_VQ85) were generated from two *Pten*$^{pc-/-}$ *Spry2*$^{pc-/+}$ tumor-bearing endpoint mice at 6 and 8 months, respectively. Cell lines were routinely grown *in vitro* in media (RPMI for PC3 and PC3M, and DMEM for P1, SP1, and SP2) supplemented with 10% FBS and 2 mmol/L glutamine.

All siRNA and plasmid transfection experiments in PC3 cells were performed using nucleofection (Lonza-kit V; see supplementary information for details). For stable *SPRY2* KD, a 19-mer SPRY2 target sequence (5′-AACACCAATGAGTACACAGAG-3; Qiagen) was used to generate CL1 and CL10 cells, and for the control a 19-mer NSi control sequence (Qiagen) was used. Stable expression of ShSPRY2 and ShNSi in human PC3 cells was achieved using a plasmid pTER+ to insert the sequence of interest and selected using zeocin (300 μg/mL).

In vivo metabolomics

Frozen prostate tumor tissues were homogenized in ice-cold extraction solution (MeOH:Acetonitrile:Water; 50:30:20; 20 mg tissue/mL) using a Precellys homogeniser (Bertin Instruments). Blood metabolites were studied by extracting whole blood in ice-cold extraction solution (1/50 ratio). All samples were centrifuged (10 minutes; 16,000*g*) and the supernatant was analyzed by high-performance LC-MS (HPLC-MS) as described below.

In vitro metabolite extractions for metabolomics

Cells were washed 3 times with ice-cold PBS and metabolites were extracted in 1 mL (nontracing studies), or 600 μL (tracing studies) extraction solution. Cell extracts were centrifuged (10 minutes; 16,000*g*) and the supernatant was analyzed by HPLC-MS as below. Data were normalized using cell-counts obtained from parallel wells, treated identically.

$^{13}C_6$-arginine tracing

PC3 (Nsi, CL1 and CL10) cells were seeded in 6-well plates (1×10^5 cells/well; 3 wells per experimental condition) in DMEM (Thermo Fisher Scientific) supplemented with 10% FBS and 2 mmol/L glutamine. Cells were allowed to proliferate for 72 hours, after which, medium was replaced with 7 mL SILAC DMEM (Silantes, catalog no. 280001300; supplemented with 10% FBS; 2 mmol/L glutamine; 0.798 mmol/L lysine) containing $^{12}C_6$-arginine (0.398 mmol/L; Sigma, catalog no. A6969) or $^{13}C_6$-arginine (0.398 mmol/L; Cambridge Isotope Lab Inc, catalog no. CLM2265-H-1). After 24 hours, metabolites were extracted as described above.

$^{13}C_1$-creatine tracing

PC3 CL1 cells were seeded in 6-well plates (7.5×10^4 cells/well; 3 wells per experimental condition) in RPMI (Thermo Fisher Scientific) supplemented with 10% FBS and 2 mmol/L glutamine (day 0). After 48 hours (day 2), medium was changed to RPMI supplemented with 10% dialyzed FBS (Sigma, catalog no. F0392) and 2 mmol/L glutamine. On day 3, medium was changed to 7 mL RPMI (10% dialyzed FBS, 2 mmol/L glutamine) in the presence/absence of ^{13}C-creatine (0.1 mmol/L; Cambridge Isotope Lab Inc, catalog no. CLM-7933-PK), and various concentrations of cyclocreatine (0, 0.1, 1, 10, and 50 mmol/L). After 24 hours, metabolites were extracted as described above.

HPLC-MS

Cell and tissue extracts were analyzed by HPLC-MS using an Orbitrap mass spectrometer (Exactive/Q Exactive Plus; Thermo Fisher Scientific) coupled with a Thermo Ultimate 3000 high-performance liquid chromatography system. The HPLC setup was equipped with a Zic-pHILIC column (SeQuant; 150 mm by 2.1 mm, 5 μm; Merck KGaA) and Zic-pHILIC guard column (SeQuant; 20 mm by 2.1 mm), and metabolites were separated on a 15-minute gradient as previously described (21). Data were acquired using Xcalibur software (v4.3, Thermo Scientific) and analyzed using Tracefinder (v4.1, Thermo Scientific).

Data availability

Raw data for this study were generated at the Metabolomics Core Facility, Beatson Institute. Derived data supporting the findings of this study are available from the corresponding author upon request.

Results

Concurrent loss of PTEN and SPRY2 mediates prostate cancer progression

Alterations of the tumor suppressors *PTEN* and *SPRY2* are observed in multiple clinical cohorts (Supplementary Fig. S1A), with heterozygous and homozygous genomic deletions of *PTEN* and *SPRY2* occurring in up to half of metastatic prostate cancers (**Fig. 1A**;

refs. 5, 22). Using a murine model of prostate cancer, we have previously shown that heterozygous loss of *Pten* and *Spry2* cooperate to drive prostate cancer progression and treatment resistance (4, 5). To investigate the functional cooperation of *Spry2* deficiency with homozygous deletion of *Pten*, we generated a prostate-specific *Pten* null mouse model with heterozygous or homozygous deletion of *Spry2* using a conditional Cre-loxP system driven by *Probasin-Cre* (5). The overall survival of mice with complete deletion of *Pten* and *Spry2* ($Pten^{pc-/-}$ $Spry2^{pc-/-}$) was significantly shorter than mice with deletion of *Pten* ($Pten^{pc-/-}$) alone, deletion of *Spry2* ($Spry2^{pc-/-}$) alone or *Pten* deletion with heterozygous loss of *Spry2* ($Pten^{pc-/-}$ $Spry2^{pc-/+}$; **Fig. 1B**). As observed before, *Spry2* loss alone did not lead to tumor formation (5). At the study endpoint, *Pten* null mice with single or double copy loss of *Spry2* had significantly higher prostate tumor burden compared with mice with *Pten* deletion alone (**Fig. 1C**; Supplementary Fig. S1B). *Pten* and *Spry2* null ($Pten^{pc-/-}$ $Spry2^{pc-/-}$) tumors were also highly proliferative as indicated by the increased Ki67 staining compared with the other genotypes (**Fig. 1D** and **E**).

Primary murine prostate cancer SP1 and SP2 cell lines were derived from two independent $Pten^{pc-/-}$ $Spry2^{pc-/+}$ double mutant tumors, and were confirmed to have suppressed *Spry2* expression (**Fig. 1F**; Supplementary Fig. S1C). As observed in murine tumors, SP1 and SP2 cells proliferated significantly faster than cells derived from a *Pten* null tumor (P1; **Fig. 1G**). Thus, concurrent loss of PTEN and SPRY2 tumor suppressors enhances murine prostate tumorigenesis with increased cell proliferation. Similarly, in PTEN deficient human PC3 prostate cancer cells, stable knockdown of *SPRY2* expression (CL1 and CL10) significantly promoted colony formation capacity when grown in soft agar (**Fig. 1H** and **I**; Supplementary Fig. S1D).

Intracellular creatine is increased upon PTEN and SPRY2 deficiency and creatine availability affects proliferation of prostate cancer cells

We next tested whether there was evidence of metabolic rewiring in tumors driven by concurrent loss of PTEN and SPRY2. Untargeted metabolomics indicated altered creatine metabolism in $Pten^{pc-/-}$ $Spry2^{pc-/-}$ tumors, with three directly related metabolites (i.e., creatine, creatine phosphate/phosphocreatine, and creatinine) being markedly elevated in murine prostate tumors with suppressed *Pten* and *Spry2* expression (when compared with tumors driven by *Pten* loss alone), as well as in *SPRY2* deficient PC3 cells (when compared with control PC3 cells; Supplementary Table S1). In addition, there was indication of increased arginine and glycine (both precursor molecules for *de novo* creatine biosynthesis, Supplementary Fig. S2A) upon loss of PTEN and SPRY2 expression in PC3 cells. Further targeted analysis confirmed significant enrichment of intracellular creatine in SPRY2 deficient human and murine prostate cancer cells (**Fig. 2A** and **B**).

Creatine can be synthesised *de novo* from glycine and arginine. To test the contribution of *de novo* synthesis to intracellular creatine in these cells, we traced the metabolic fate of $^{13}C_6$-arginine in PC3 Nsi, CL1 and CL10 cells (Supplementary Fig. S2A). We observed clear evidence for uptake of labelled arginine (Supplementary Fig. S2B) and active arginine metabolism, as indicated by the production of $^{13}C_6$-argininosuccinate [a metabolite arising from reverse activity of argininosuccinate lysase as shown previously (21); Supplementary Fig. S2C]. Consistent with our observation, the intracellular level of creatine was increased in the SPRY2-deficient cell lines when compared with control cells. However, we observed minimal levels of $^{13}C_1$-creatine and these were similar when culturing cells with $^{13}C_6$-arginine or with $^{12}C_6$-arginine (**Fig. 2C**). This strongly suggests that any detected $^{13}C_1$-creatine was due to natural abundance of ^{13}C-carbons rather than *de novo* synthesis.

Creatine can also be taken up from the environment via the specific creatine transporter (CRT/SLC6A8; ref. 23) and we found its gene expression significantly increased in both murine and human prostate cancer cells deficient for SPRY2 (**Fig. 2D** and **E**). Stable knockdown of *SLC6A8* in SPRY2 deficient PC3 cells (**Fig. 2F**) significantly decreased cellular creatine levels (**Fig. 2G**), and impaired colony formation in a soft agar assay (**Fig. 2H**).

To investigate if creatine availability can control tumor growth *in vivo*, we tested the impact of creatine supplementation in six months old $Pten^{pc-/-}$ $Spry2^{pc-/-}$ mice. A 2-month treatment with creatine significantly increased the proliferation of prostate tumors as shown by Ki67 staining (**Fig. 2I** and **J**; Supplementary Fig. S2D).

Collectively, these data indicate that creatine availability and uptake affects prostate tumor growth driven by SPRY2-deficiency. In the Memorial Sloan Kettering Cancer Center (MSKCC; New York, NY) clinical prostate cancer cohort (cBioPortal; ref. 24), patients with high *SLC6A8* expression were at risk of disease progression (**Fig. 2K**), and expression of *SPRY2* and *PTEN* negatively correlated with *SLC6A8* expression (Supplementary Fig. S2E and S2F). Across 24 clinical prostate cancer cohorts, alteration (mainly copy-number amplification) of *SLC6A8* was associated with significantly shorter patient survival, and tends to be observed in patient cohorts of advanced (metastatic or treatment resistant) disease (Supplementary Fig. S2G and S2H). In addition, upregulated *SLC6A8* expression was associated with multiple known prostate cancer oncogenes implicated in lethal disease, possibly via the function of its putative transcription factors (Supplementary Table S2A, with Supplementary Table S2B showing co-occurrence between altered *FOXA1* and *SLC6A8* in specific cohorts).

Cyclocreatine suppresses creatine metabolism and proliferation in prostate cancer cells

Cyclocreatine is a creatine analogue that has been shown to functionally block the phosphagen system (25, 26). While cellular uptake of cyclocreatine is reported to be mediated by SLC6A8 (27), it remains to be investigated whether cyclocreatine exerts its effects via inhibition of creatine synthesis and/or uptake. We tested the effect of cyclocreatine (varying concentrations up to 1%) on the *in vitro* proliferative capacity of murine and human prostate cancer cells with varying SPRY2 expression. Cyclocreatine (1%) impaired *in vitro* proliferation of both human and murine prostate cancer cells (**Fig. 3A** and **B**). A dose dependent response to cyclocreatine treatment was observed with growth inhibition detected at a dose as low as 0.125% (Supplementary Fig. S3A–S3F). Furthermore, cyclocreatine treatment significantly impaired the colony-forming ability of PC3 cells (**Fig. 3C**), along with reduced cellular creatine and phosphocreatine levels (**Fig. 3D** and **E**) while leaving ATP levels unaltered (**Fig. 3F**). Together these data suggest cyclocreatine may have potential as a therapeutic agent for prostate cancer.

To directly study how cyclocreatine affects creatine uptake and metabolism, we performed stable isotope tracing using ^{13}C-creatine (0.1 mmol/L), in the presence/absence of cyclocreatine (0.1 mmol/L to 50 mmol/L, with 50 mmol/L being 0.7% cyclocreatine). Cyclocreatine was efficiently internalized by PC3 CL1 cells (**Fig. 4A**). We observed a dose-dependent inhibition of ^{13}C-creatine uptake (**Fig. 4B**), and production of the related metabolites ^{13}C-creatinine and ^{13}C-phosphocreatine (**Fig. 4C** and **D**). Collectively, our data show that, when exogenously available to these cells, the main source of

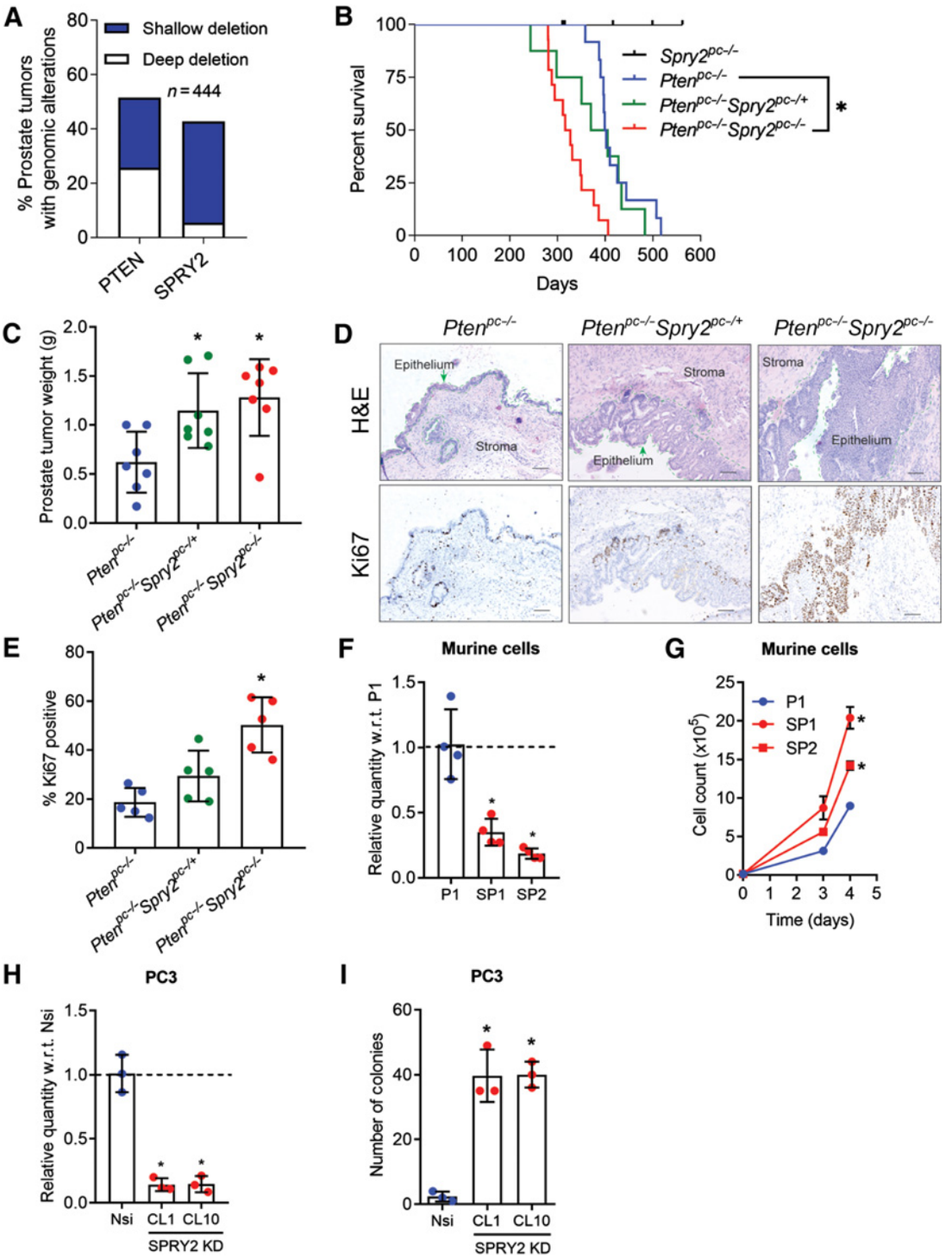

Figure 1.

Concomitant PTEN and SPRY2 deficiencies drive prostate cancer progression. **A,** *PTEN* and *SPRY2* genomic alterations in patients with metastatic prostate cancer (SU2C/PCF Dream Team, PNAS 2019; ref. 41). **B,** Kaplan–Meier plot for overall survival of indicated mice $Spry2^{pc-/-}$, $n = 5$; $Pten^{pc-/-}$, $n = 12$; $Pten^{pc-/-}$ $Spry2^{pc-/+}$, $n = 8$; $Pten^{pc-/-}$ $Spry2^{pc-/-}$, $n = 14$ (*, $P < 0.0001$, $Pten^{pc-/-}$ $Spry2^{pc-/-}$ compared with $Pten^{pc-/-}$; $P = 0.0021$, $Pten^{pc-/-}$ $Spry2^{pc-/-}$ compared with $Spry2^{pc-/-}$; $P = 0.0274$, $Pten^{pc-/-}$ $Spry2^{pc-/-}$ compared with $Pten^{pc-/-}$ $Spry2^{pc-/+}$; log-rank Mantel-Cox test). **C,** Noncystic prostate tumor weights from indicated mice at clinical endpoints ($n = 7$ mice for each group. Mean values ± SD are shown. *, $P < 0.05$ compared with $Pten^{pc-/-}$; one-way ANOVA with Tukey multiple comparison test. **D,** Representative hematoxylin and eosin (H&E) and Ki67 images of prostate tumor sections from $Pten^{pc-/-}$, $Pten^{pc-/-}$ $Spry2^{pc-/+}$, and $Pten^{pc-/-}$ $Spry2^{pc-/-}$ mice ($n = 5$ mice for each group). Scale bar, 100 μm. (*Continued on the following page.*)

intracellular creatine is via uptake, a process that is impaired by cyclocreatine.

Cellular creatine and creatine kinases are components of the phosphagen system (28), which serves as a cellular energy buffering system to quickly generate ATP on demand (22). By efficiently storing high energy phosphates as phosphocreatine, the phosphagen system may promote tumorigenesis, especially in rapidly proliferating tumors with high energy demands. Because creatine can stimulate mitochondrial respiration in certain tissues (29), we investigated the effect of creatine on cellular respiration. Creatine treatment significantly increased basal respiration in SPRY2 deficient PC3 cells (CL1 and CL10; **Fig. 4E–G**). The creatine kinase activity (namely generation of phosphocreatine and ADP from creatine and ATP) was elevated in SPRY2 deficient cells, and suppressed in all cell lines by cyclocreatine (Supplementary Fig. S3G). Despite increased creatine kinase activity and creatine induced basal respiration, the total cellular ATP and phosphocreatine levels were not altered in SPRY2 deficient cells (Supplementary Fig. S3H and S3I).

Effects of cyclocreatine on *in vivo* prostate carcinogenesis and metastatic potential

To investigate the tumor suppressive effects of cyclocreatine, we treated prostate tumor bearing $Pten^{pc-/-}$ $Spry2^{pc-/-}$ mice with 1% cyclocreatine for one month. Treatment was well tolerated and we did not observe evidence of any cyclocreatine-related pathologies as indicated by normal mouse weights and histological examination of the major organs (namely heart, kidney, liver, and spleen; Supplementary Table S3; Supplementary Fig. S4A). Cyclocreatine treatment significantly decreased tumor cell proliferation as shown by reduced Ki67 staining (**Fig. 5A** and **B**), while the trend for reduced tumor weights did not reach statistical significance (**Fig. 5C**). We next performed metabolic analysis of tumor tissues and whole blood, collected from control or cyclocreatine-treated animals. Cyclocreatine was detected in both blood (**Fig. 5D**) and tumor tissues (**Fig. 5E**), confirming that the drug had reached the tissue of interest. Further data analysis showed alterations in creatine metabolism upon cyclocreatine treatment. Whereas no changes were observed in the steady-state level of creatine (**Fig. 5F**) or phosphocreatine (**Fig. 5G**), the intratumoral levels of its breakdown product creatinine (**Fig. 5H**) were significantly decreased. Furthermore, cyclocreatine increased the arginine levels, and decreased guanidinoacetate levels in tumors (**Fig. 5I** and **J**). Such metabolic alterations would be in line with inhibition of *de novo* creatine synthesis. Although we could not demonstrate *de novo* synthesis of creatine in human prostate cancer cells cultured *in vitro* (**Fig. 2C**), these observations may indicate synthesis in one or more cell populations within the tumor microenvironment *in vivo*. The observed changes in the tumoral levels of arginine or guanidinoacetate were not observed in the blood samples (Supplementary Fig. S4B and S4C), but a systemic effect of cyclocreatine affecting intratumoral metabolites cannot be ruled out.

Regardless of the tumor genotype, the process of cancer metastasis is metabolically demanding in terms of both energy and biomass. We therefore tested the effect of cyclocreatine in a model of liver metastasis, which may affect patients with advanced and treatment refractory prostate cancer. To this purpose, splenic injections of PC3M cells were performed and mice were treated with 1% cyclocreatine for a month. Liver metastatic burden was significantly reduced by cyclocreatine (**Fig. 5K** and **L**).

Overall, our data highlight the importance of creatine in prostate cancer, and reveal new molecular insights into the mechanism of cyclocreatine treatment on creatine metabolism, with creatine uptake being the dominant source.

Discussion

Metabolic adaptations in cancers (including prostate cancer) may contribute to progressive tumor growth. Understanding such oncogenic metabolic alterations can expose tumor-specific vulnerabilities that can be exploited for cancer therapy. Hence, we investigated the metabolic changes observed in prostate cancer driven by clinically relevant deficiency of PTEN and SPRY2. Building on previous research (4, 5), combined loss of the tumor suppressors PTEN and SPRY2 was found to further enhance tumor growth and progression. Here we show that creatine availability supports the growth of PTEN and SPRY2 deficient prostate cancer, while cyclocreatine impairs creatine uptake and metabolism, and thereby suppresses proliferation. (A summary of *P* values from statistical analysis is presented in Supplementary Table S4.)

Diet is a major source of creatine. Circulating creatine can enter cells via the bidirectional SLC6A8 creatine transporter. Upregulated SLC6A8 expression in PTEN and SPRY2 deficient prostate cancer cells helps to maintain elevated cellular creatine levels required for enhanced proliferation. Of note, the strong correlation between *SLC6A8* expression and patient survival observed across multiple clinical cohorts highlights the importance of creatine availability in progressive prostate cancer irrespective of the underlying molecular drivers (not being limited to tumors driven by the combined loss of PTEN and SPRY2). While integration of multiple datasets in a single analysis increases the confidence of the overall analysis, dataset biases and batch effects between cohorts may influence the outcome. Future research characterizing SLC6A8 protein expression by IHC in clinical prostate cancer samples is required to identify the subpopulations of prostate cancer patients with tumor-specific upregulation of SLC6A8, and to determine whether SLC6A8 protein expression correlates with patient survival.

The molecular mechanism responsible for upregulated SLC6A8 expression in progressive prostate cancer remains to be formally investigated. Several well described oncogenes for prostate cancer, including but not restricted to *AR*, *ERG1*, *FOXA1* (Supplementary Table S2A and S2B), are strongly associated with upregulated *SLC6A8* expression. Furthermore, the *SLC6A8* promoter sequence contains

(*Continued.*) **E,** IHC quantification of Ki67 in prostate tumors as indicated ($n = 5$ mice for each group). Mean values ± SD are shown. *, $P < 0.05$ compared with $Pten^{pc-/-}$; one-way ANOVA with Tukey multiple comparison test. **F,** Relative mRNA levels of *Spry2* in primary murine prostate cancer cells as indicated. P1 derived from $Pten^{pc-/-}$; SP1 and SP2 derived from two independent $Pten^{pc-/-}$ $Spry2^{pc-/+}$ prostate tumors ($n = 4$ independent experiments). Mean values ± SD are shown. *, $P < 0.05$ compared with P1; one-way ANOVA with Dunnett multiple comparison test. **G,** Growth of indicated cells ($n = 3$ independent experiments). Mean values ± SEM are shown. *, $P < 0.05$ compared with P1; two-way ANOVA with Tukey multiple comparison test. **H,** Relative mRNA levels of *SPRY2* in PC3 human prostate cancer cell lines as indicated. Nsi is PC3 cells with stable expression of nonsilencing vector control; CL1 and CL10 are PC3 clones with stable knockdown (KD) of SPRY2 ($n = 3$ independent experiments). Mean values ± SD are shown. *, $P < 0.05$ compared with Nsi; one-way ANOVA with Dunnett multiple comparison test. **I,** Soft agar colony quantifications of the indicated cells. Data shown are from a single representative experiment, performed three times with three technical replicates each. Mean values ± SD are shown. *, $P < 0.05$ compared with Nsi; one-way ANOVA with Dunnett multiple comparison test.

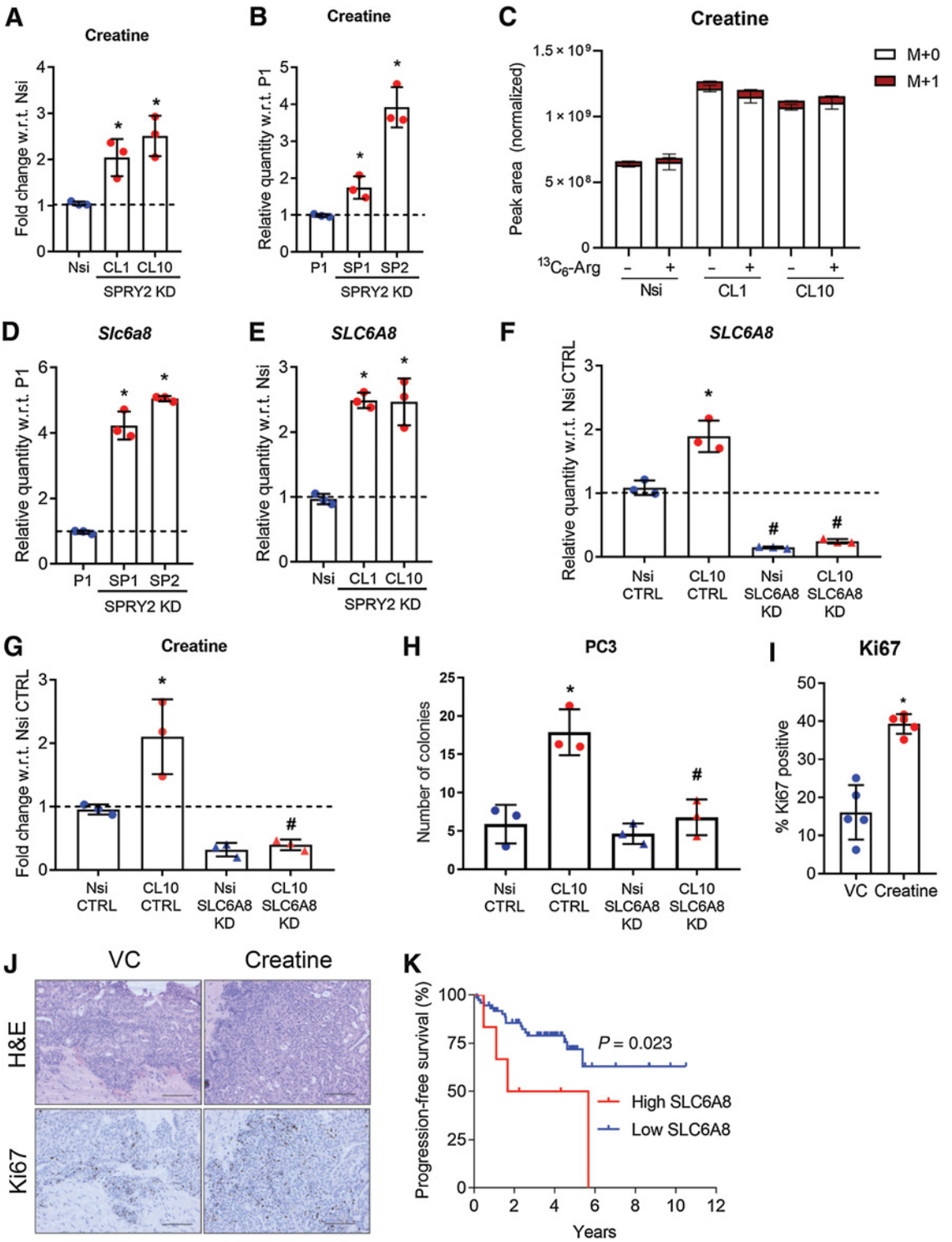

Figure 2.

Creatine availability affects proliferation of prostate cancer cells and is increased upon PTEN and SPRY2 deficiency. **A** and **B,** Relative cellular creatine levels in human (**A**) and murine prostate cancer cells ($n = 3$ independent experiments; **B**). Mean values ± SD are shown. *, $P < 0.05$ compared with Nsi and P1, respectively; unpaired t test. **C,** Intracellular abundance of creatine isotopes (M+0, M+1) in PC3 cells (Nsi, CL1, and CL10) after 24-hour incubation in the presence of unlabeled arginine or $^{13}C_6$-arginine. Data from single experiment with three technical replicates per condition. Mean values ± SD. **D,** Relative levels of creatine transporter *Slc6a8* mRNA in murine prostate cancer cells. Data shown are from a single representative experiment, performed three times with three technical replicates each. Mean values ± SD are shown. *, $P < 0.05$ compared with P1; one-way ANOVA with Dunnett multiple comparison test. (*Continued on the following page.*)

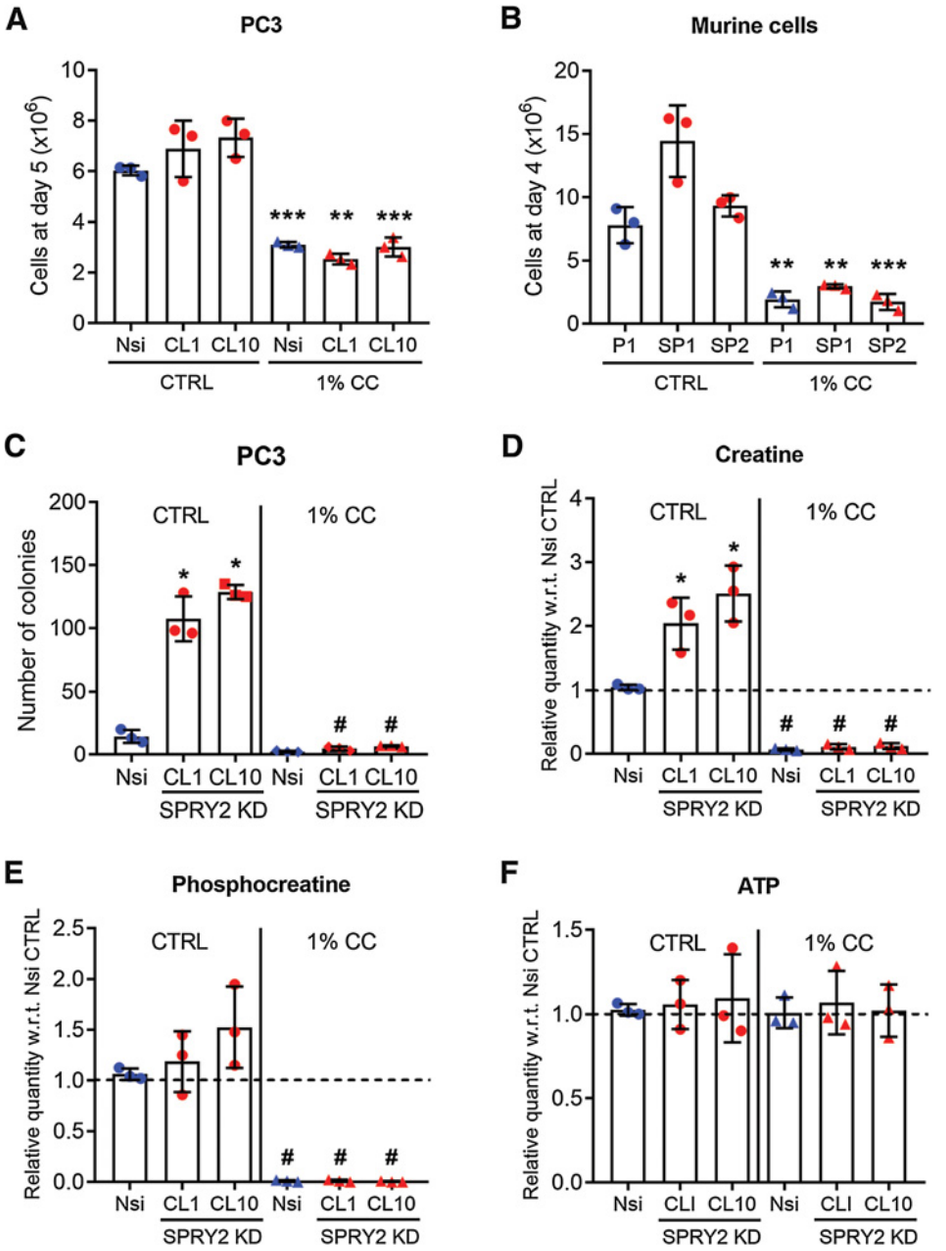

Figure 3.

Cyclocreatine suppresses creatine metabolism and proliferation in prostate cancer cells. **A** and **B,** *In vitro* growth of human PC3 (**A**) and murine (**B**) cells treated with control (CTRL) or 1% cyclocreatine (CC; $n = 3$ independent experiments). Mean values ± SD are shown. **, $P < 0.005$; ***, $P < 0.0005$ comparing cyclocreatine treatment with respective CTRL cells; unpaired *t* test. **C,** Soft agar colony quantifications of PC3 Nsi and SPRY2 KD clones (CL1 and CL10) treated with control or 1% cyclocreatine containing medium. Data shown from a single representative experiment performed twice, with three technical replicates each. Mean values ± SD are shown. *, $P < 0.05$ compared with Nsi CTRL and #, $P < 0.05$ compared with respective CTRL cells; one-way ANOVA with Tukey multiple comparison test. **D–F,** Relative levels of cellular creatine (**D**), phosphocreatine (**E**), and ATP in control (CTRL; **F**) or 1% cyclocreatine-treated PC3 Nsi and SPRY2 KD clones CL1 and CL10 ($n = 3$ independent experiments). Mean values ± SD are shown. *, $P < 0.05$ compared with Nsi CTRL and #, $P < 0.05$ compared with respective CTL cells; one-way ANOVA with Tukey multiple comparison test.

putative binding sites for a number of transcription factors including E2F-1, E2F-2, E2F-3a, EGR-4, and SP1 (source: genecards.org). We observed significant associations between each of the putative transcription factors and upregulated *SLC6A8* expression (Supplementary Table S2A). Collectively, these data highlight the potential for multiple oncogenic pathways to stimulate creatine metabolism via regulation of *SLC6A8* expression, thereby supporting cancer progression. To directly test the role of various transcription factors in *SLC6A8* transcription,

(*Continued.*) **E,** Relative levels of creatine transporter *SLC6A8* in human prostate cancer cells ($n = 3$ independent experiments). Mean values ± SD are shown. *, $P < 0.05$ compared with Nsi; one-way ANOVA with Dunnett multiple comparison test. **F,** Relative levels of *SLC6A8* mRNA in PC3 Nsi and SPRY2 KD CL10 with SLC6A8 KD ($n = 3$ independent experiments). Mean values ± SD are shown. *, $P < 0.05$ compared with Nsi CTRL and #, $P < 0.05$ compared with respective CTL cells; one-way ANOVA with Tukey multiple comparison test. **G,** Relative cellular creatine levels in PC3 Nsi and SPRY2 KD CL10 with SLC6A8 KD ($n = 3$ independent experiments). Mean values ± SD are shown *, $P < 0.05$ compared with Nsi CTRL and #, $P < 0.05$ compared with respective CTL cells; one-way ANOVA with Tukey multiple comparison test. **H,** Number of soft agar colonies of PC3 Nsi and SPRY2 KD CL10 with SLC6A8 KD ($n = 3$ independent experiments). Mean values ± SD are shown. *, $P < 0.05$ compared with Nsi CTRL and #, $P < 0.05$ compared with respective CTRL cells; one-way ANOVA with Dunnett multiple comparison test. **I,** IHC quantification of Ki67 in prostate tumors from $Pten^{pc-/-}$ $Spry2^{pc-/-}$ mice treated for 2 months with vehicle (VC) or 1% creatine ($n = 5$ mice for each group). Mean values ± SD are shown. *, $P < 0.05$; Mann–Whitney test. **J,** Representative hematoxylin and eosin (H&E) and Ki67 images of prostate tumor sections from $Pten^{pc-/-}$ $Spry2^{pc-/-}$ mice treated for 2 months with vehicle (VC) or 1% creatine. $n = 5$ mice for each group. Scale bar, 100 µm. **K,** Kaplan–Meier plot for progression-free survival in MSKCC, Cancer Cell 2010 (24) prostate cancer dataset showing cases with high (more than z-score = 1.8; $n = 6$) or low (less than z-score = 1.8; $n = 74$) expression of *SLC6A8*; log-rank Mantel-Cox test.

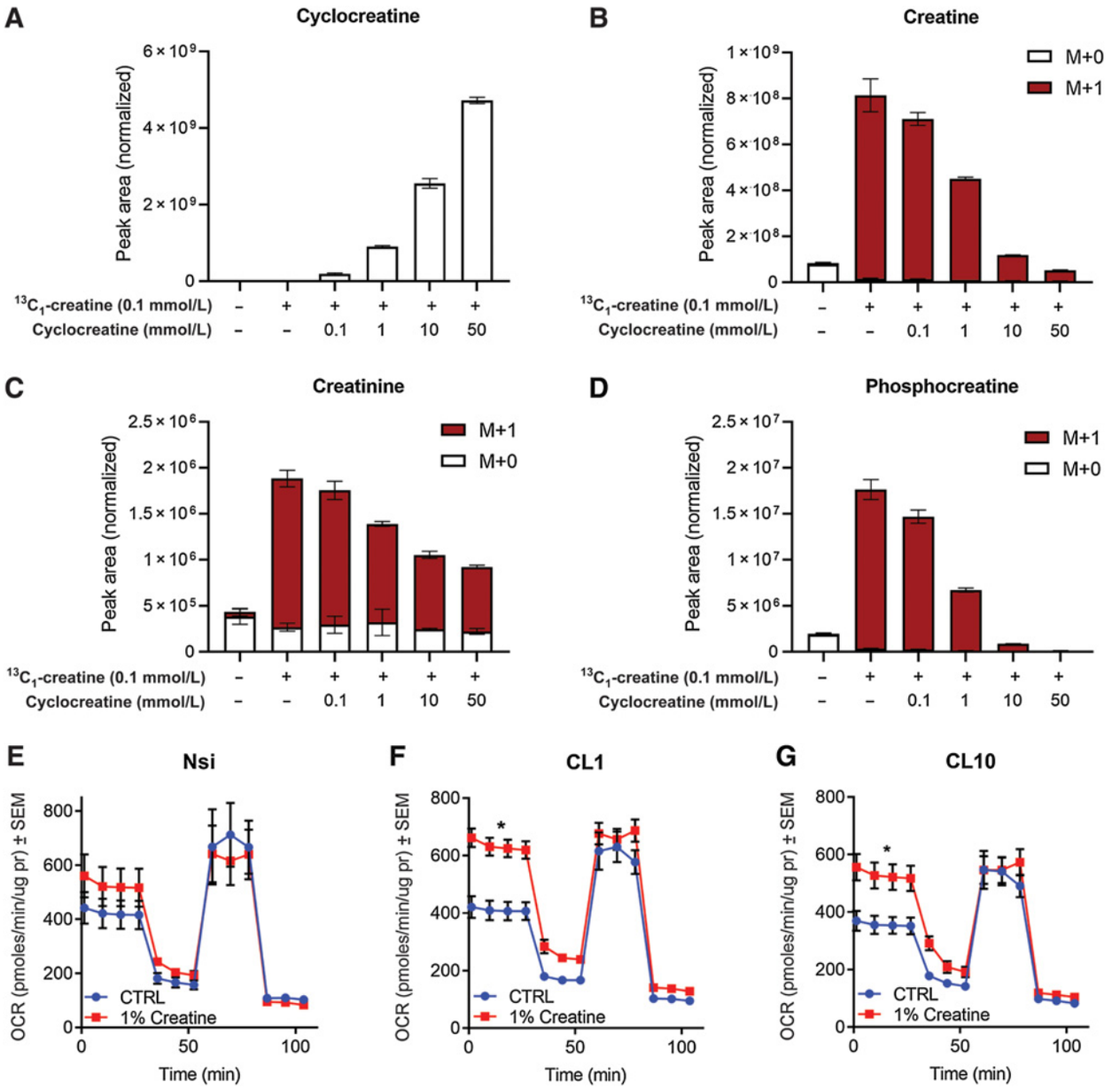

Figure 4.

Cyclocreatine suppresses creatine uptake and metabolism. **A,** Intracellular abundance of cyclocreatine in PC3 CL1 cells after 24 hours treatment with various concentrations of cyclocreatine and ^{13}C-creatine. Data are from single experiment with three technical replicates per condition. Mean values ± SD are shown. **B–D,** Intracellular abundance of different isotopes of creatine (**B**), creatinine (**C**), and phosphocreatine (M+0, M+1; **D**) in PC3 CL1 cells after 24 hours treatment with various concentrations of cyclocreatine and ^{13}C-creatine. Data are from single experiment with three technical replicates per condition. Mean values ± SD are shown. **E–G,** Oxygen consumption rate in PC3 Nsi (**E**), SPRY2 KD CL1 (**F**), and SPRY2 KD CL10 (**G**) treated as indicated ($n = 4$ independent experiments). Mean values ± SEM are shown. *, $P < 0.05$ compared with CTRL; two-way ANOVA with Tukey multiple comparison test.

formal chromatin immunoprecipitation sequencing experiments along with experimental validation of transcriptional control will be required.

Prostate tumors driven by inactivation of PTEN and SPRY2 harbor synergistic concurrent activation of the RAS/ERK and PI3K/AKT pathways, with evidence of functional interactions with multiple molecular events including inactivation of PP2A as a tumor suppressor (5) or activation of HER2 as an oncogene (3). HER2 mediated oncogenic signals can promote mitochondrial creatine kinase stability to enhance cellular bioenergetics (with increased phosphocreatine and cellular ATP availability; refs. 30, 31). In line with this, we observed increased creatine kinase activity in PTEN and SPRY2 deficient prostate cancer cells; however, no alterations in the overall levels of phosphocreatine and ATP were detected in PTEN- and SPRY2-deficient cells. This may reflect the dynamic flux of the phosphagen system and tightly regulated nature of cellular energy homeostasis, but

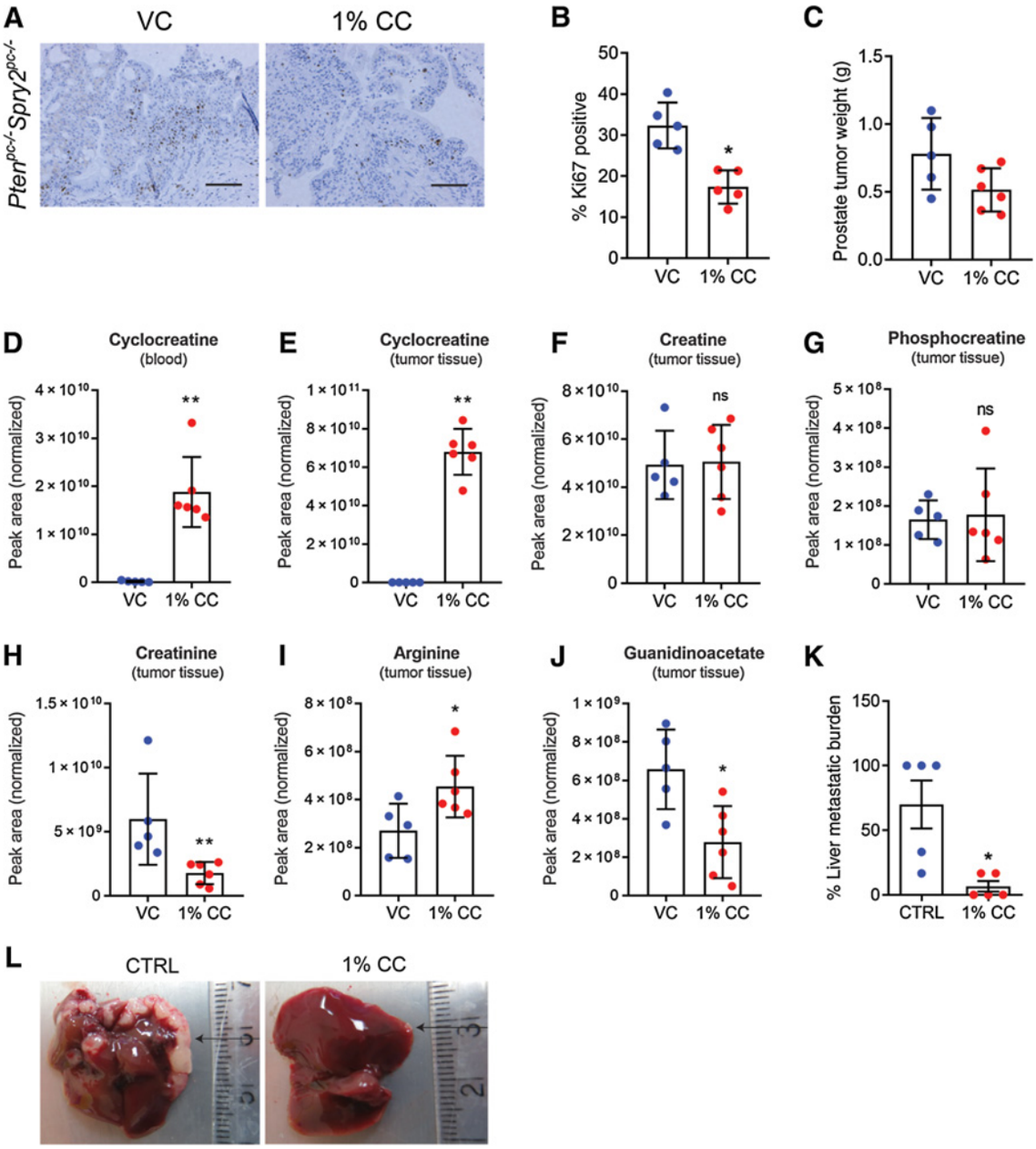

Figure 5.

Cyclocreatine treatment affects prostate cancer progression *in vivo*. **A,** Representative Ki67 images of prostate tumor sections from $Pten^{pc-/-}$ $Spry2^{pc-/-}$ mice treated for 1 month with vehicle (VC) or 1% cyclocreatine (CC; $n = 5$ mice for each group). Scale bar, 100 μm. **B,** IHC quantification of Ki67 in prostate tumors from $Pten^{pc-/-}$ $Spry2^{pc-/-}$ mice treated for 2 months with vehicle or 1% cyclocreatine ($n = 5$ mice for each group). Mean values ± SD are shown. *, $P < 0.05$; Mann–Whitney test. **C,** Noncystic prostate tumor weights from $Pten^{pc-/-}$ $Spry2^{pc-/-}$ mice treated for 1 month with vehicle ($n = 5$) or 1% cyclocreatine ($n = 6$); mean values ± SD are shown. **D,** Cyclocreatine abundance detected in whole blood of $Pten^{pc-/-}$ $Spry2^{pc-/-}$ mice treated with 1% cyclocreatine ($n = 6$) or vehicle ($n = 5$). Data show mean ± SD. **, $P < 0.01$; Mann–Whitney test. **E–J,** Abundance of cyclocreatine (**E**), creatine (**F**), phosphocreatine (**G**), creatinine (**H**), arginine (**I**), and guanidinoacetate (**J**) detected in tumor tissues of $Pten^{pc-/-}$ $Spry2^{pc-/-}$ mice treated with 1% cyclocreatine ($n = 6$) or vehicle ($n = 5$). Data show mean ± SD. **, $P < 0.01$; Mann–Whitney test. **K,** Percentage PC3M liver metastases burden in CD-1 nude mice treated with control or 1% cyclocreatine water (*ad libitum*) for 1 month ($n = 5$ mice for each group). Mean values ± SEM are shown. *, $P < 0.05$; Mann–Whitney test. **L,** Representative images of PC3M liver metastases in CD-1 nude mice treated with control or 1% cyclocreatine water (*ad libitum*) for 1 month ($n = 5$ mice for each group). Arrows, liver metastases.

also supports recent reports (12, 32, 33) showing a functional role of creatine metabolism beyond energy buffering and ATP generation.

To date, detailed analysis of how cyclocreatine treatment impacts on creatine metabolism has been lacking. Our metabolic analyses using stable isotope labelling revealed the importance of reduced creatine uptake because of cyclocreatine treatment. Together with emerging literature on the role of the creatine transporter SLC6A8 in progressive colorectal (34) and breast cancer (35), our data add to the therapeutic

potential of suppressing creatine uptake and metabolism in prostate cancer. It is worth noting that while *de novo* synthesis of creatine was not observed in prostate cancer cells when cultured *in vitro* (**Fig. 2C**), our metabolic analysis of tumor tissues cannot confidently exclude active creatine synthesis (and inhibition thereof by cyclocreatine) in the various cell populations within the tumor microenvironment *in vivo*. Functional interactions among multiple cell populations within the tumor microenvironment substantially increase the complexity of *in vivo* tumor metabolism. In support of metabolic cross-talk within the tumor microenvironment, creatine synthesis by peritumoral adipocytes was recently found to fuel breast cancer progression via altered downstream tumoral lipid metabolism (36). Similarly, in pancreatic cancer, stroma-associated stellate cells and tumor-associated macrophages support tumor progression or treatment resistance, via release of key metabolites, namely alanine (37) and pyrimidines (38) respectively. Future mechanistic investigation of metabolic cross-talk within the prostate tumor microenvironment and its effect on creatine availability could include: (i) Analysis of creatine synthesis/metabolism in cancer-associated stromal and immune cells, and (ii) Modulation of SLC6A8 activity in genetically engineered mouse models (GEMM) of prostate cancer. A GEMM driving increased *Slc6a8* expression would test whether this increases intracellular creatine levels and promotes tumor progression, including metastasis. On the other hand, genetic deletion or pharmacologic SLC6A8 inhibition (e.g., using RGX-202) (34), in a progressive prostate cancer model (e.g., *Pb-Pten*$^{fl/fl}$ *Spry2*$^{fl/fl}$, *Pb-Pten*$^{fl/fl}$ *Ctnnb*$^{+/fl}$; ref. 39) would inform whether decreased SLC6A8 activity suppresses tumorigenesis.

In prostate cancer, the concept of resistance training is being considered to tackle androgen deprivation therapy induced loss of lean body mass. Hence, creatine supplementation is studied as an ongoing lifestyle intervention in a clinical trial for prostate cancer (19). Our observation of increased cellular proliferation in tumors from *Pten*$^{pc-/-}$ *Spry2*$^{pc-/-}$ mice following creatine supplementation for only eight weeks highlights the need to assess creatine supplementation in patients with prostate cancer with caution. Consistent with our findings, dietary uptake, or GATM-mediated *de novo* synthesis of creatine, enhanced cancer metastasis and shortened mouse survival via upregulated Snail and Slug expression in a Smad2 and Smad3 dependent manner in *in vivo* models of breast and colorectal cancer (14, 40).

Overall, we show that SPRY2 and PTEN double deficient prostate cancer cells sustain growth by engaging creatine metabolism. Furthermore, cyclocreatine mediated blockade of the phosphagen system and produced anti-proliferative effects regardless of the status of SPRY2. Therapies such as cyclocreatine that target the phosphagen system may bring about antitumor effects through suppressed creatine uptake, likely to be important in clinical prostate tumors with increased SLC6A8 creatine transporter expression.

Authors' Disclosures

L.K. Rushworth reports grants from Cancer Research UK during the conduct of the study. O.J. Sansom reports grants from AstraZeneca, Cancer Research Technology, Novartis, and grants from RedX outside the submitted work. No disclosures were reported by the other authors.

Authors' Contributions

R. Patel: Conceptualization, supervision, investigation, methodology, writing–original draft. **C.A. Ford:** Data curation, validation, investigation, methodology, writing–original draft, writing–review and editing. **L. Rodgers:** Formal analysis, investigation, writing–review and editing. **L.K. Rushworth:** Data curation, validation, methodology, writing–original draft, project administration, writing–review and editing. **J. Fleming:** Formal analysis, methodology. **E. Mui:** Resources, data curation, formal analysis, methodology, project administration. **T. Zhang:** Formal analysis, writing–review and editing. **D. Watson:** Resources, data curation, formal analysis, supervision, methodology, writing–review and editing. **V. Lynch:** Formal analysis, supervision, visualization, methodology. **G. Mackay:** Resources, formal analysis, supervision, investigation, methodology. **D. Sumpton:** Resources, data curation, formal analysis, supervision, validation, methodology, writing–review and editing. **O.J. Sansom:** Resources, investigation, methodology, writing–review and editing. **J. Vande Voorde:** Conceptualization, data curation, formal analysis, supervision, investigation, methodology, writing–original draft, writing–review and editing. **H.Y. Leung:** Conceptualization, resources, supervision, funding acquisition, investigation, methodology, writing–original draft, project administration, writing–review and editing.

Acknowledgments

This work was supported by Cancer Research UK: A17196 - core funding to the CRUK Beatson Institute; A15151 awarded to H.Y. Leung; A21139, A25045, A17196, and A31287 awarded to O.J. Sansom. L. Rodgers received a CRUK Clinical Research Fellowship (A19493). The authors thank Colin Nixon for support with histology input and Arnaud Blomme for useful discussion.

The costs of publication of this article were defrayed in part by the payment of page charges. This article must therefore be hereby marked *advertisement* in accordance with 18 U.S.C. Section 1734 solely to indicate this fact.

Received May 4, 2021; revised February 16, 2022; accepted May 18, 2022; published first June 8, 2022.

References

1. Siegel RL, Miller KD, Jemal A. Cancer statistics, 2020. CA Cancer J Clin 2020;70:7–30.
2. Lohiya V, Aragon-Ching JB, Sonpavde G. Role of chemotherapy and mechanisms of resistance to chemotherapy in metastatic castration-resistant prostate cancer. Clin Med Insights Oncol 2016;10:57–66.
3. Gao M, Patel R, Ahmad I, Fleming J, Edwards J, McCracken S, et al. SPRY2 loss enhances ErbB trafficking and PI3K/AKT signaling to drive human and mouse prostate carcinogenesis. EMBO Mol Med 2012;4:776–90.
4. Patel R, Fleming J, Mui E, Loveridge C, Repiscak P, Blomme A, et al. Sprouty2 loss-induced IL6 drives castration-resistant prostate cancer through scavenger receptor B1. EMBO Mol Med 2018;10:e8347.
5. Patel R, Gao M, Ahmad I, Fleming J, Singh LB, Rai TS, et al. Sprouty2, PTEN, and PP2A interact to regulate prostate cancer progression. J Clin Invest 2013;123:1157–75.
6. Hanahan D, Weinberg RA. Hallmarks of cancer: the next generation. Cell 2011;144:646–74.
7. Fenouille N, Bassil CF, Ben-Sahra I, Benajiba L, Alexe G, Ramos A, et al. The creatine kinase pathway is a metabolic vulnerability in EVI1-positive acute myeloid leukemia. Nat Med 2017;23:301–13.
8. Patra S, Ghosh A, Roy SS, Bera S, Das M, Talukdar D, et al. A short review on creatine-creatine kinase system in relation to cancer and some experimental results on creatine as adjuvant in cancer therapy. Amino Acids 2012;42:2319–30.
9. Wallimann T. Bioenergetics: dissecting the role of creatine kinase. Curr Biol 1994;4:42–6.
10. Wyss M, Kaddurah-Daouk R. Creatine and creatinine metabolism. Physiol Rev 2000;80:1107–213.
11. Bera S, Wallimann T, Ray S, Ray M. Enzymes of creatine biosynthesis, arginine and methionine metabolism in normal and malignant cells. FEBS J 2008;275:5899–909.
12. Kazak L, Cohen P. Creatine metabolism: energy homeostasis, immunity, and cancer biology. Nat Rev Endocrinol 2020;16:421–36.
13. Qian XL, Li YQ, Gu F, Liu FF, Li WD, Zhang XM, et al. Overexpression of ubiquitous mitochondrial creatine kinase (uMtCK) accelerates tumor growth by inhibiting apoptosis of breast cancer cells and is associated with a poor prognosis in breast cancer patients. Biochem Biophys Res Commun 2012;427:60–6.
14. Zhang L, Zhu Z, Yan H, Wang W, Wu Z, Zhang F, et al. Creatine promotes cancer metastasis through activation of Smad2/3. Cell Metab 2021;33:1111–23.

15. Bylsma LC, Alexander DD. A review and meta-analysis of prospective studies of red and processed meat, meat cooking methods, heme iron, heterocyclic amines and prostate cancer. Nutr J 2015;14:125.
16. Iwasaki M, Tsugane S. Dietary heterocyclic aromatic amine intake and cancer risk: epidemiological evidence from Japanese studies. Genes Environ 2021;43:33.
17. Ollberding NJ, Wilkens LR, Henderson BE, Kolonel LN, Le Marchand L. Meat consumption, heterocyclic amines and colorectal cancer risk: the Multiethnic Cohort Study. Int J Cancer 2012;131:E1125–33.
18. Kreider RB, Stout JR. Creatine in health and disease. Nutrients 2021;13:447.
19. Fairman CM, Kendall KL, Newton RU, Hart NH, Taaffe DR, Chee R, et al. Examining the effects of creatine supplementation in augmenting adaptations to resistance training in patients with prostate cancer undergoing androgen deprivation therapy: a randomized, double-blind, placebo-controlled trial. BMJ Open 2019;9:e030080.
20. Gardner JR, Livingston PM, Fraser SF. Effects of exercise on treatment-related adverse effects for patients with prostate cancer receiving androgen-deprivation therapy: a systematic review. J Clin Oncol 2014;32:335–46.
21. Vande Voorde J, Ackermann T, Pfetzer N, Sumpton D, Mackay G, Kalna G, et al. Improving the metabolic fidelity of cancer models with a physiological cell culture medium. Sci Adv 2019;5:eaau7314.
22. Abida W, Cyrta J, Heller G, Prandi D, Armenia J, Coleman I, et al. Genomic correlates of clinical outcome in advanced prostate cancer. Proc Natl Acad Sci USA 2019;116:11428–36.
23. Christie DL. Functional insights into the creatine transporter. Subcell Biochem 2007;46:99–118.
24. Taylor BS, Schultz N, Hieronymus H, Gopalan A, Xiao Y, Carver BS, et al. Integrative genomic profiling of human prostate cancer. Cancer Cell 2010;18:11–22.
25. Kornacker M, Schlattner U, Wallimann T, Verneris MR, Negrin RS, Kornacker B, et al. Hodgkin disease-derived cell lines expressing ubiquitous mitochondrial creatine kinase show growth inhibition by cyclocreatine treatment independent of apoptosis. Int J Cancer 2001;94:513–9.
26. Lillie JW, O'Keefe M, Valinski H, Hamlin HA Jr, Varban ML, Kaddurah-Daouk R. Cyclocreatine (1-carboxymethyl-2-iminoimidazolidine) inhibits growth of a broad spectrum of cancer cells derived from solid tumors. Cancer Res 1993;53:3172–8.
27. Uemura T, Ito S, Masuda T, Shimbo H, Goto T, Osaka H, et al. Cyclocreatine transport by SLC6A8, the creatine transporter, in HEK293 cells, a human blood-brain barrier model cell, and CCDSs patient-derived fibroblasts. Pharm Res 2020;37:61.
28. Ellington WR. Evolution and physiological roles of phosphagen systems. Annu Rev Physiol 2001;63:289–325.
29. Kazak L, Chouchani ET, Jedrychowski MP, Erickson BK, Shinoda K, Cohen P, et al. A creatine-driven substrate cycle enhances energy expenditure and thermogenesis in beige fat. Cell 2015;163:643–55.
30. Ben-Sahra I, Puissant A. HER2 signaling hijacks the creatine shuttle to fuel breast cancer cell growth. Cell Metab 2018;28:805–7.
31. Kurmi K, Hitosugi S, Yu J, Boakye-Agyeman F, Wiese EK, Larson TR, et al. Tyrosine phosphorylation of mitochondrial creatine kinase 1 enhances a druggable tumor energy shuttle pathway. Cell Metab 2018;28:833–47.
32. Kazak L, Rahbani JF, Samborska B, Lu GZ, Jedrychowski MP, Lajoie M, et al. Ablation of adipocyte creatine transport impairs thermogenesis and causes diet-induced obesity. Nat Metab 2019;1:360–70.
33. Tang X, Keenan MM, Wu J, Lin CA, Dubois L, Thompson JW, et al. Comprehensive profiling of amino acid response uncovers unique methionine-deprived response dependent on intact creatine biosynthesis. PLoS Genet 2015;11:e1005158.
34. Kurth I, Yamaguchi N, Andreu-Agullo C, Tian HS, Sridhar S, Takeda S, et al. Therapeutic targeting of SLC6A8 creatine transporter suppresses colon cancer progression and modulates human creatine levels. Sci Adv 2021;7:eabi7511.
35. Li Q, Liu M, Sun Y, Jin T, Zhu P, Wan X, et al. SLC6A8-mediated intracellular creatine accumulation enhances hypoxic breast cancer cell survival via ameliorating oxidative stress. J Exp Clin Cancer Res 2021;40:168.
36. Maguire OA, Ackerman SE, Szwed SK, Maganti AV, Marchildon F, Huang X, et al. Creatine-mediated cross-talk between adipocytes and cancer cells regulates obesity-driven breast cancer. Cell Metab 2021;33:499–512.
37. Sousa CM, Biancur DE, Wang X, Halbrook CJ, Sherman MH, Zhang L, et al. Pancreatic stellate cells support tumor metabolism through autophagic alanine secretion. Nature 2016;536:479–83.
38. Halbrook CJ, Pontious C, Kovalenko I, Lapienyte L, Dreyer S, Lee HJ, et al. Macrophage-released pyrimidines inhibit gemcitabine therapy in pancreatic cancer. Cell Metab 2019;29:1390–9.
39. Patel R, Brzezinska EA, Repiscak P, Ahmad I, Mui E, Gao M, et al. Activation of beta-catenin cooperates with loss of Pten to drive AR-independent castration-resistant prostate cancer. Cancer Res 2020;80:576–90.
40. Zhang L, Bu P. The two sides of creatine in cancer. Trends Cell Biol 2022;32:380–90.
41. Abida W, Cyrta J, Heller G, Prandi D, Armenia J, Coleman I, et al. Genomic correlates of clinical outcome in advanced prostate cancer. Proc Natl Acad Sci U S A 2019;116:11428–36.